Science of the Total Environment 601–602 (2017) 821–832

Contents lists available at ScienceDirect

Science of the Total Environment

journal homepage: www.elsevier.com/locate/scitotenv

Spatio-temporal topsoil organic carbon mapping of a semi-arid Mediterranean region: The role of land use, soil texture, topographic indices and the influence of remote sensing data to modelling

Calogero Schillaci [a,b], Marco Acutis [a], Luigi Lombardo [b,c,d], Aldo Lipani [e], Maria Fantappiè [f], Michael Märker [b,g], Sergio Saia [h,*]

[a] Department of Agricultural and Environmental Science, University of Milan, Italy
[b] Department of Geosciences, University of Tübingen, Germany
[c] PSE Division, King Abdullah University of Science and Technology, Thuwal, Saudi Arabia
[d] CEMSE Division, King Abdullah University of Science and Technology, Thuwal, Saudi Arabia
[e] Institute of Software Technology and Interactive Systems, TU Wien, Austria
[f] Council for Agricultural Research and Economics (CREA), Centre for Agrobiology and Pedology (CREA-ABP), Florence, Italy
[g] Department of Earth and Environmental Sciences, University of Pavia, Italy
[h] Council for Agricultural Research and Economics (CREA), Cereal Research Centre (CREA-CER), Foggia, Italy

HIGHLIGHTS

- Modelling SOC in two samplings 15 year apart gave a view of SOC change.
- Texture and land use were main drivers of SOC concentration.
- Topographic indices were more important than climatic indices to estimate SOC concentration.
- SOC variation agreed with climatic trend and soil variability maps.
- Remote sensing covariates reduced the uncertainty of estimation.

GRAPHICAL ABSTRACT

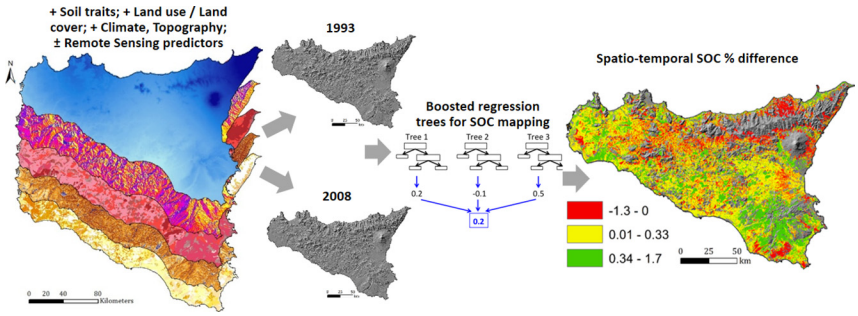

ARTICLE INFO

Article history:
Received 4 January 2017
Received in revised form 21 May 2017
Accepted 25 May 2017
Available online xxxx

Editor: D. Barcelo

Keywords:
SOC mapping
Space-time SOC variation
Agro-ecosystems
R programming

ABSTRACT

SOC is the most important indicator of soil fertility and monitoring its space-time changes is a prerequisite to establish strategies to reduce soil loss and preserve its quality. Here we modelled the topsoil (0–0.3 m) SOC concentration of the cultivated area of Sicily in 1993 and 2008. Sicily is an extremely variable region with a high number of ecosystems, soils, and microclimates. We studied the role of time and land use in the modelling of SOC, and assessed the role of remote sensing (RS) covariates in the boosted regression trees modelling. The models obtained showed a high pseudo-R^2 (0.63–0.69) and low uncertainty (s.d. < 0.76 g C kg^{-1} with RS, and <1.25 g C kg^{-1} without RS). These outputs allowed depicting a time variation of SOC at 1 arcsec. SOC estimation strongly depended on the soil texture, land use, rainfall and topographic indices related to erosion and deposition. RS indices captured one fifth of the total variance explained, slightly changed the ranking of variance explained by the non-RS predictors, and reduced the variability of the model replicates. During the study period, SOC decreased in the areas with relatively high initial SOC, and increased in the area with high temperature and low rainfall, dominated by arables. This was likely due to the compulsory application of some Good Agricultural and Environmental practices. These results confirm that the importance of texture and land use in short-term SOC variation is

* Corresponding author.
E-mail address: sergio.saia@crea.gov.it (S. Saia).

http://dx.doi.org/10.1016/j.scitotenv.2017.05.239

Digital soil mapping
Legacy dataset

comparable to climate. The present results call for agronomic and policy intervention at the district level to maintain fertility and yield potential. In addition, the present results suggest that the application of RS covariates enhanced the modelling performance.

1. Introduction

Agricultural lands play a major role in the storage of soil organic carbon (SOC) and sequestration/release of atmospheric CO_2 (Bradford et al., 2016; Filippi et al., 2016; Post and Kwon, 2000). SOC is directly linked with a number of ecosystem services and agronomical benefits and is the main driver of soil fertility. However, agricultural soils have been depleted from their original SOC stock due to cultivation, which also negatively affected soil aggregation status, water infiltration rate, soil fertility and biota (Bruun et al., 2015; Parras-Alcántara et al., 2016; Saia et al., 2014). The preservation of soil quality is a priority to maintain agricultural productivity and environmental quality. In this framework, monitoring SOC concentration and stock changes through space and time is important to establish strategies to reduce soil loss and preserve its quality. SOC monitoring at regional scale relies on sparse sampling and application of an estimation process. Such a process should take into account the spatial interdependence of samples and abundance of predictors (Martin et al., 2014); and the distribution heterogeneity in space and among determinants (predictors) of SOC accumulation (Lacoste et al., 2014). With regards to the latter, the relationship in the domain of each predictor with SOC and the resolution of the predictors is particularly relevant for any spatial estimation (Miller et al., 2016; Miller et al., 2015a; Miller et al., 2015b). The spatial estimation of SOC concentration and stocks is commonly performed by statistical approaches (Meersmans et al., 2009; Orton et al., 2014) with different interpolation methods and machine learning predictive models (Henderson et al., 2005; Yang et al., 2015). The former is better suited to areas with dense SOC measurements, whereas the second is more appropriate for non-regularly sampled regions, since its outcome does not rely on the sample proximity to extract functional (ecological) relationships between dependent and independent variables.

SOC dynamics under different land uses are still poorly understood (Francaviglia et al., 2017; Meersmans et al., 2008; Purton et al., 2015), especially when deriving data from wide areas and with different climates. In Mediterranean environment, lack of knowledge on SOC dynamic is further due to variable climatic and erratic meteorological conditions. It has been shown that cultivation exerts a negative role on SOC accumulation in various environments (Francaviglia et al., 2017; Kämpf et al., 2016; Novara et al., 2013) and this likely depends on both soil tillage and reduction of biomass return to the soil. In particular, a reduction of the tillage intensity can favor SOC accumulation irrespective of aridity (from semi-arid to humid) and can be up to 1 t SOC ha^{-1} yr^{-1} (Conant et al., 2001; Kämpf et al., 2016; Kurganova et al., 2014; Post and Kwon, 2000). The SOC dynamic also depends on other factors such as soil genesis and type, land use history and management and useful information could be gained from SOC spatial models (Badagliacca et al., 2017; Martin et al., 2014; Schillaci et al., 2017; Schillaci et al., 2015; Vereecken et al., 2016).

In the last two decades the integration of physical, chemical, and biological information derived from different covariates in the models has boosted the studies on soil properties (Bui et al., 2009; Henderson et al., 2005) and also for SOC mapping from global or continental (Hengl et al., 2014; Lugato et al., 2014) to regional and plot scales (Akpa et al., 2016; de Gruijter et al., 2016; Martin et al., 2014; Schillaci et al., 2017). SOC mapping attempts at giving an image of the spatial distribution despite it is costly (Minasny et al., 2013 and reference therein).

The most recent developments in the digital soil mapping include machine learning (Forkuor et al., 2017; Gasch et al., 2015; Hengl et al., 2017) to study space-time variation of soil properties and use of remote sensing (RS) covariates (Castaldi et al., 2016a). Thanks to their high accessibility, resolution and availability for wide areas, RS data gained importance for spatial prediction of the topsoil organic C (Bou Kheir et al., 2010; Poggio et al., 2013). For example, Bou Kheir et al. (2010) found that SOC maps built with a classification-tree analysis of the sole RS parameters gave the same accuracy of a model built with sole digital elevation model (DEM) parameters, and both of them had sole ca. 10% less accuracy that a full RS + DEM + soil parameters model built. Poggio et al. (2013) found that integration of RS with terrain attribute data increased the predictive ability comparing to the model built with only terrain parameters. However, some of the SOC estimates lack uncertainty analysis and this compromises the reliability of predictions for decision making (Maia et al., 2010; Minasny et al., 2013; Ogle et al., 2010). In addition, Conant et al. (2011) highlighted the limitation to document time changes in SOC because of the spatial variability in the factors that influence SOC distribution.

In a regularly-spaced data collection, SOC samples are taken from representative or random sampling sites in a given study area. Legacy data comes from a mixture of sampling campaigns resulting in data collected for different aims (Chartin et al., 2017), which frequently allow to make predictions for areas with sampling limitations (Rial et al., 2017). Depending on the scope of each survey (e.g. regional soil characterization or precision agriculture) sample density can change abruptly. This can consist in drawbacks including their non-regular distribution in space, which call for the use of particular modelling method and predictors. Due to these difficulties, only few examples on mapping at regional extent with legacy data are available. For example, Ross et al. (2013) and Grinand et al. (2017) carried out a space-time assessment of SOC in subtropical regions of south-eastern United States and Madagascar, respectively.

Little information is available on SOC dynamics in semi-arid Mediterranean areas due to the unavailability of consistent databases. Nonetheless, time dynamic of SOC storage in the soil is highly dependent to the climatic zone of the area under study (Doetterl et al., 2015). In addition, spatial and time change of SOC can respond to different determinants at varying the climate of area under study.

The present work fits within the big picture of spatial SOC mapping and time change. This was made by means of a legacy dataset and use of remotely sensed data. In particular, we used legacy data of two sampling campaigns 15 years apart (1993–2008), coupled with climate (from Worldclim data Bio1,12), and land use information (from CORINE 1990 to 2006) to map the topsoil SOC variation across time in the agricultural area of a semi-arid Mediterranean region (Fig. 1). Such aim was achieved by applying a machine learning method, namely boosted regression trees (BRT), to each sampling campaign dataset using land use, soil texture, topographic and remote sensing predictors. We also tested the role of remote sensing covariates in the spatial SOC prediction and predictors' importance by running each model either with or without the implementation of the RS covariates. In the area under study, i.e. cropped fields in which plants (mostly field crops) have limited or no growth during summer and early fall, the inclusion of remote sensed variables could capture part of the SOC variation due to biomass return to the soil.

2. Material and methods

2.1. Study area

The study area, Sicily (Italy), is a semiarid region located in middle of the Mediterranean Sea (Fig. 1). Its area is about 25,286 km^2, 60% of

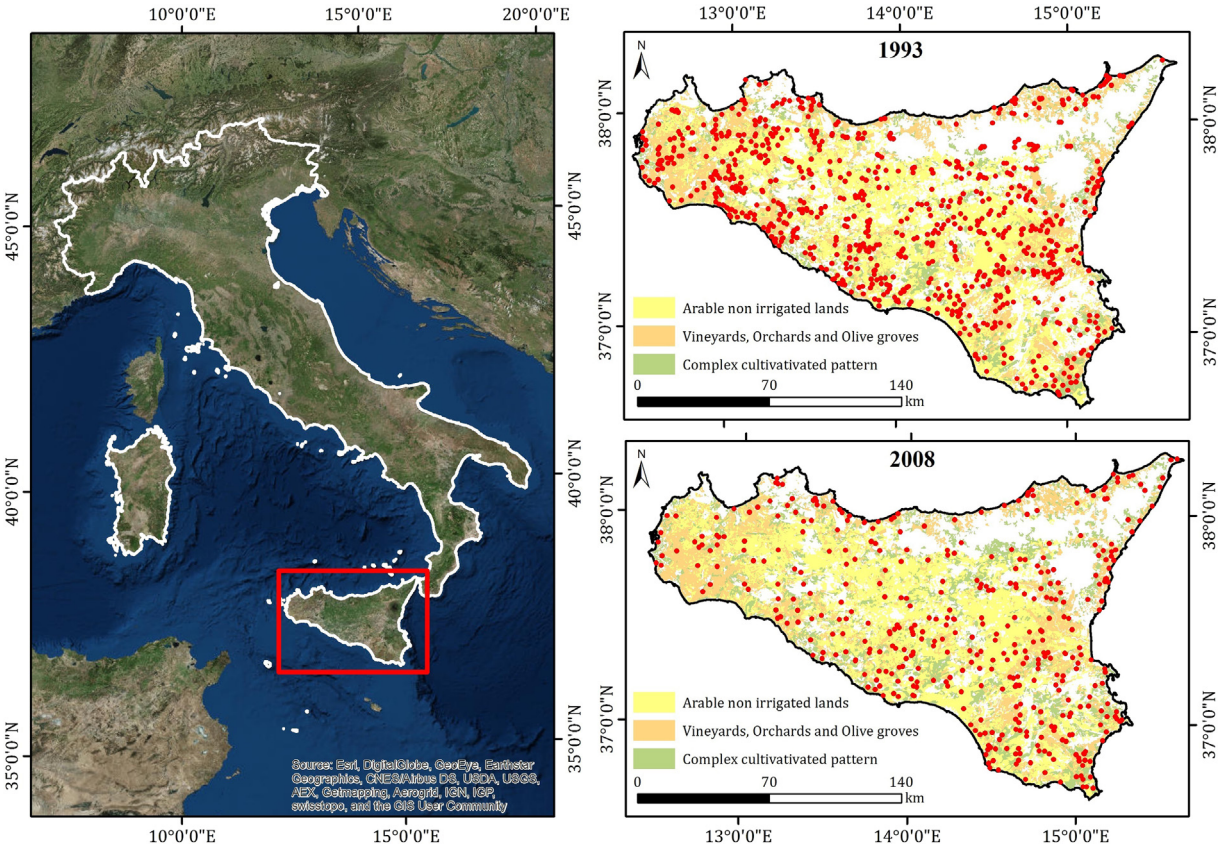

Fig. 1. Locations of the sampling sites in the 1993 and 2008 in the area under study (Sicily, Italy). Land use groups used in the study are displayed.

which cultivated. The macroclimate of the region is Mediterranean with three main bioclimatic areas: thermo-, meso-, and supra-Mediterranean. Mean annual temperatures in the cropped area range from 7 °C to 15 °C and mean annual precipitation from 350 to 1000 mm, whereas mean annual temperatures and rainfall in the natural, uncropped area can be 1.8 °C and up to 1300 mm (Cannarozzo et al., 2006; Viola et al., 2014). The main annual crops are durum wheat, winter-seeded barley, pulses and forage legumes and a wide range of horticultural crops; the main perennial crops are olive groves, vineyards and fruit trees such as citrus, almonds, and stone fruits. Woodlands and secondary forests are not targeted by the SOC concentration mapping in the present work, except those areas in which agriculture abandonment occurred.

Adoption of conservation soil management techniques is almost absent (Ruisi et al., 2014). In the region, different soil survey campaigns were undertaken between 1968 and 2008. The criteria for the selection of the locations of the soil sampling are explained in the next section. The island has a great pedoclimatic variability: dominant soils according to the World Reference Base for soils are Calcaric Regosols, Haplic Calcisols, Calcic Vertisols, Vitric or Silandic Andosols, Calcaric and/or Mollic Leptosols, Calcaric Phaeozems, and Fluvic Cambisols. Hence it can be considered quite representative of most of the Mediterranean countries. A number of ecological and anthropic traits make Sicily unique for ecological studies. These traits include a relatively high population density and degree of cultivation, an ancient environmental history, climatic variability, land uses and several dominations from different populations, which introduced various plant species and management techniques. All these factors made Sicily an open and extremely variable laboratory for the study of the impact of anthropic pressure and environmental variation at microscale, land cultivation and management on other environmental traits, including SOC distribution and dynamics. Such characteristics strongly help in the exportation of the results of environmental studies to other similar and different environments and scale, such as also suggested by others (Legendre, 1998; Novara et al., 2017; Schmolke et al., 2010).

The region under study, Sicily (see Supplementary material Fig. 1 for a physiographic map of the area with orography and toponymy information used), is a setting of different agro-ecosystems and natural environments though it is mainly semi-arid and with few incidence of forestlands. The island has three main, almost continuous, mountain chains: Peloritani from the north-eastern corner moving to west few km down the northern coast, followed by the Nebrodi and then by the Madonie. In the western/central part of the island there is an irregular mountain area: the Sicani, somehow continuing the ridge formed by the previous mountain chains. Mean height of the mountain chains decreases from east to west. These chains were formed as part of the Apennines, which span across the island as a geological bridge between peninsular Italy (on the east end) and Tunisia (on the west end). The highest mountain of Sicily is the Etna Volcano (about 3600 m above sea level [a.s.l.]), located in the northeastern part of the region, south of the Peloritani. To the south of the Etna Volcano, a wide plain (the Catania plain) is formed by the alluvium of the Simeto River, south of which there is the expansion of a hilly to mountainous area: the Hyblaean mountains/plateau. The rest of the core of the island, from the plain of Catania to the Erei Mountains and cities of Enna, Caltanissetta and Agrigento is a mostly hilly area with clayey, high pH, seldom gipsic saline soils. Such as for the main mountain chains, mean height of this latter ridge decreases from east to west. Other minor plains can be retrieved all along the coasts. All the rivers, with the exception above-mentioned Simeto, have a strong seasonal flow. This is due to the low rainfall south of the Apennines ridge, or low basin extent north of it.

2.2. SOC dataset

The Regional Bureau for Agriculture, Rural Development and Mediterranean Fishery, the Department of Agriculture, and Service 7

UOS7.03 provided the legacy dataset used in this study. The surveys that produced the legacy dataset had different aims (such as redaction of suitability or pedological maps). SOC, soil texture, actual land use, GPS positioning and relative metadata were measured in every survey and provided for the present work. From the complete record of observation (about 2700 different locations in a timespan of 30 years), we selected the years with the most of samplings, which were 1993 (685 points) and 2008 (337 points) (Fig. 1). The 1993 database is a regional subset of the national soil survey performed in the framework of the AGRIT project of the Italian Ministry of Agriculture and Forestry (MIPAAF), all over Italy in the years 1993 to 1994. The 2008 campaign (undertaken in the frame of the project "Soil Map of Sicily at 1:250,000 scale") was aimed at closing the gap of previous campaigns basing on a GIS oriented pedo-landscape sampling design (Fantappiè et al., 2011). Only SOC data sampled in agricultural fields were taken into account for further modelling procedures.

In both the 1993 and 2008 campaigns, soil-sampling scheme was designed to collect samples from various pedo-landscape (combinations of physiographies, lithologies and land uses) delineations as representative at a 1:250,000 scale. Samples of the 1993 campaign were taken following a specific guide for soil sampling and description, and consisted of minipits excavated up to a 50 cm depth to represent the top-soil, and sampled with the auger for the subsoil. The 2008 campaign consisted of soil profiles described according to the official methods of Italian Ministry of Agriculture (Paolanti et al., 2010). Soils from each campaign were sampled at various depths (maximum depth sampled up to 2.80 m). For the present study, the topsoil layer (up to 0.3-m depth) was taken into account. As stated above, soil layers were sampled according to the pedological description and thus upper and lower limit of each depth sampled varied among sampling points. Thus, to standardize the SOC concentration value, SOC was considered to decrease linearly with depth within each layers. In particular, soil layer in the depth 0–0.3 m were selected and those deeper than 50 cm were not used for the present experiment. The soil samples were passed through a 2 mm sieve, air dried, then analyzed for organic C content following Walkley-Black procedure.

2.3. Predictors

Climatic data were drawn from Worldclim (Hijmans et al., 2005). The original resolution of the Climatic data is about 1 km and were resampled to the desired 100 m mapping unit for the modelling process. Worldclim offers different datasets including bioclimatic data. Mean yearly rainfall and temperature of the 1950–2010 period were used.

Soil texture was obtained by the sedimentation method of the samples and reported according to the USDA classification. Soil texture for the whole area was provided by the Regional Bureau for Agriculture, Rural Development and Mediterranean Fishery, the Department of Agriculture, Service 7 UOS7.03 Geographical Information Systems, Cartography and Broadband Connection in Agriculture, Palermo.

The **CORINE land cover maps** of the years 1990 and 2006 at 100-m spatial resolution were used in order to identify the agricultural land uses for the model built for the year 1993 and 2008, respectively (http://land.copernicus.eu/pan-european/corine-land-cover). The analysis was carried out according to the CORINE level 3, the Land cover type used in the modelling stage were: i) non-irrigated arable land (CORINE code 2.1.1, grid code 12, hereafter referred as ARA), ii) vineyards (CORINE code 2.2.1, grid code 15), fruit trees and berry plantations (CORINE code 2.2.2, grid code 16), and olive groves (CORINE code 2.2.3, grid code 17) (hereafter grouped in VFO), iii) annual crops associated with permanent crops (CORINE code 2.4.1, grid code 19), complex cultivation patterns (CORINE code 2.4.2, grid code 20), land principally occupied by agriculture, with significant areas of natural vegetation (CORINE code 2.4.3, grid code 21) (hereafter grouped in CCP). The land uses within the groups VFO and CCP were grouped since the SOC stock and relationship between SOC-predictors and SOC stock in these land uses is very similar due to similarities in plant density and soil management, as observed in Schillaci et al. (2017). CORINE codes are provided in Supplementary material Table 1.

Remote sensing-derived predictors consisted of the LANDSAT 5 spectral bands. The imagery was also used to derive the Normalized Difference Vegetation Index (NDVI), which was included as explanatory variables in the modelling phase. We used geometrical corrected images L1G. Multi-temporal mosaic required normalization to adjust for inconsistencies between images because of the proximity of the sun, earth and zenith angle. The procedure involved the conversion of the digital number to radiance at sensor. Calibration coefficient was provided in the imagery metadata (Guyot and Gu, 1994). The images used for the study were obtained by mosaicking the following five LANDSAT 5 scenes using the only cloud free scenes belonging to the path 188 row 33 (East), path 198 row 33 and 34 (middle) and path 190 row 33 and 34 (West) from the 1987 and 2003 for modelling data of 1993 and 2008, respectively. This time differences (1987 for the 1993 and 2003 for the 2008) were needed since the regional extent of the study area requires at least 3 LANDSAT path to make a complete mosaicking of the region and these years were the closer to those of the sampling periods, in which the satellites scenes close each other in time had no or very few clouds, thus allowing a homogeneous dataset. LANDSAT imagery was freely acquired from the United States Geological Survey catalogue (USGS, http://earthexplorer.usgs.gov) and coincided with summer period (Rouse Jr. et al., 1974), when most of the field crops have stubble or bare soil and very few or no crop growth occurs in other crops due to extremely high temperature and low water availability. All the RS predictors had an original spatial resolution of 30 m and they have been subsequently resampled to the desired 100 m mapping unit. The choice of such predictor is due to their strong linkage to vegetation and other soil traits, and thus, to SOC.

2.4. Topographical indices

Shuttle Radar Topography Mission (SRTM-C) digital elevation model (DEM) released in September 2014 with a 1-arcsec (30 m) spatial resolution (resampled to 100 m to fit the land use classification) was used for the calculation of the morphometric spatial predictors by means of SAGA GIS (Conrad et al., 2015). DEM was downloaded from the earthexplorer.com website, then pre-processing such as mosaicking and fill sink was applied to the 10 SRTM DEM tiles covering the regional extent. Eleven terrain attributes were calculated: 1) slope 2) catchment area, 3) aspect, 4) plan curvature; 5) profile curvature, 6) length-slope factor, 7) channel network base level, 8) convergence index, 9) valley depth, 10) topographic wetness index, 11) landform classification. See http://www.saga-gis.org/saga_tool_doc/2.1.3/a2z.html for details on the computation of these covariates. Categorical predictor codes are provided in Supplementary material Table 1.

2.5. Boosted regression trees and map comparison

Boosted Regression Trees (BRT, Elith et al., 2008) was used to identify the relationships between SOC and its predictors and to regionalize the SOC prediction. This method and other decision trees-based models have already been used as DSM techniques to deal with SOC concentration and stock mapping (Bou Kheir et al., 2010; Grimm et al., 2008; Martin et al., 2011; Schillaci et al., 2017). BRT is based on the integration of weak learners (or tree-based rules). In a data mining context, a weak learner is defined as a model that performs just slightly better than random guessing (Freund and Schapire, 1997). In this sense, the BRT algorithm combines multiple weak learners into a single strong learner (Lombardo et al., 2015). This allow the algorithm to progressively increases the accuracy of the prediction by reducing the chance of obtaining outliers since weak learners also produces weak outliers. This additive structure allows for capturing the variance of a dependent variable in a way where the deeper the tree is grown, the more fitting

Table 1
Descriptive statistics of the observed soil organic carbon (SOC) concentration values and that of the distributions of the predicted SOC values modelled extracted on the same locations of the observed values. RS if for remote sensing covariates. Descriptive statistics were produced for both row and log-transformed data. Unit of measure for row data is % SOC.

	Raw data						Log-transformed data					
	1993			2008			1993			2008		
	Observed	Predicted with RS	Predicted without RS	Observed	Predicted with RS	Predicted without RS	Observed	Predicted with RS	Predicted without RS	Observed	Predicted with RS	Predicted without RS
Mean	1.2219	1.2246	1.2246	1.4881	1.4959	1.4965	0.0080	0.0687	0.0693	0.0743	0.1536	0.1546
Standard error	0.0273	0.0146	0.0143	0.0567	0.0249	0.0244	0.0098	0.0044	0.0044	0.0146	0.0065	0.0064
Minimum	0.1000	0.6821	0.6665	0.0300	0.8027	0.7774	−1.0000	−0.1661	−0.1762	−1.5229	−0.0955	−0.1093
Percentile 1%	0.2000	0.7322	0.7231	0.2000	0.8523	0.8889	−0.6990	−0.1354	−0.1408	−0.6990	−0.0694	−0.0512
Percentile 2.5%	0.2000	0.7779	0.7811	0.2533	0.9137	0.9222	−0.6990	−0.1091	−0.1073	−0.5965	−0.0392	−0.0352
Percentile 25%	0.8000	0.9599	0.9611	0.8325	1.1294	1.1416	−0.0969	−0.0178	−0.0172	−0.0796	0.0529	0.0575
Median	1.0000	1.1125	1.1148	1.1450	1.3573	1.3480	0.0000	0.0463	0.0472	0.0588	0.1327	0.1297
Percentile 75%	1.5000	1.3453	1.3392	1.7575	1.6973	1.7033	0.1761	0.1288	0.1268	0.2449	0.2298	0.2313
Percentile 97.5%	3.2475	2.4201	2.3855	4.4638	2.9182	2.8322	0.5115	0.3838	0.3776	0.6497	0.4651	0.4521
Percentile 99%	4.2000	2.7196	2.7162	5.6966	2.9813	3.0149	0.6232	0.4345	0.4340	0.7556	0.4744	0.4793
Maximum	5.4000	2.9830	3.0140	10.9500	3.4762	3.3565	0.7324	0.4746	0.4791	1.0394	0.5411	0.5259
Mode	1.0000	1.0554	1.0151	0.9900	0.8205	0.7774	0.0000	0.0234	0.0065	−0.0044	−0.0859	−0.1093
Standard deviation	0.7648	0.4074	0.4002	1.1530	0.5074	0.4968	0.2751	0.1237	0.1218	0.2972	0.1318	0.1294
Kurtosis	5.1596	3.4557	3.4879	14.9722	1.5478	1.5422	1.3897	0.7781	0.8042	2.1546	−0.0729	−0.0682
Skewness	1.8570	1.7964	1.7953	2.9695	1.3679	1.3563	−0.6215	0.9741	0.9742	−0.3757	0.6848	0.6774

segments are obtained and added to the initial tree, to accommodate the SOC concentration at each mapping unit. The first step of this procedure consist of a Classification And Regression Trees (CART) analysis which recursively screens the observations in matched datasets made up by a dependent variable, either categorical (classification) or continuous (regression), and one or many explanatory variables. Explanatory variables can be either categorical or continuous. Differently from a classic CART approach, where a single tree can grow only to be finally pruned to get a readable model, the application of the BRT (second step) iteratively generates trees of a fixed dimension. Each tree is based upon the previous, and BRT gradually minimizes a loss function in order to improve the predictive performance. The adoption of the Huber-M loss function instead of a more common square loss function reduces the noise when iteratively measuring the difference between estimated and actual values for SOC concentration data. The procedure ceases when the creation of trees produces overfitting effects. The evaluation of the overfitting is performed by measuring the prediction residuals or deviance for each of the consecutive trees over a random independent sample that was kept separate from the calibration phase. Typically, the testing error quickly decreases the more trees are generated and subsequently slows down reaching an inflection point from where it starts to increase. This behavior is recognized as overfitting, determining the choice of the best model before the tree starts fitting the noise of the training data instead of revealing ecological relationships.

In the present research, 100 replicates were randomly generated and modelled from each of the original SOC concentration dataset. Relationships between variables are explained through response curves (Lombardo et al., 2015). We used R (R Development Core Team, 2008), with the 'dismo' package developed by Elith et al. (2008). The package allows for the customization of: i) learning rate (lr), which is set to determine the contribution of each tree to the final tree architecture; ii) tree complexity (tc), which controls the number of splits; iii) bag of fraction (bg), the proportion of data selected at each step of the modelling procedure. Following Hashimoto et al. (2016) we performed the 10-fold cross-validation procedure to determine the optimal number of trees (maximum numbers of trees 10,000) and a tc value of 20. Regarding each single run, model performances was assessed using the coefficient of determination of the scatter plot of the predicted against the observed values (pseudo-R^2) and root mean square error (RMSE). Standard deviation maps of the 100 runs were also constructed.

The maps of organic carbon generated for the 1993 and 2008 were compared and a difference (SOC_{08}–SOC_{93}) computed in which an increase of SOC was displayed as positive and a decrease as negative. An error map of the difference was built by adding the standard error of

Table 2
The importance of each of the 25 predictors used in the boosted regression trees model to estimate the soil organic carbon performed on the 1993 and 2008 samples in Sicily, Italy. The role of the remote sensed (RS) predictors on the contribution to the total variance explained by the non-RS predictors and fold variation after removal of the RS predictors is shown.

	1993			2008		
	With RS	Without RS[a]	*Fold variation*	With RS	Without RS	*Fold variation*
Non-remote sensed (RS) predictors						
Soil texture	16.18	16.17	*1.00*	22.64	24.14	*1.07*
Land use	12.02	14.37	*1.20*	6.79	8.56	*1.26*
Valley depth	9.24	10.21	*1.10*	2.38	3.24	*1.36*
Rainfall	5.91	9.27	*1.57*	4.21	5.93	*1.41*
Channel network base level	4.97	6.96	*1.40*	9.05	10.35	*1.14*
LS factor	4.61	5.65	*1.23*	3.35	4.27	*1.28*
Landforms	4.19	5.04	*1.20*	4.44	5.34	*1.20*
Aspect	3.88	4.89	*1.26*	4.54	5.84	*1.29*
Elevation	3.38	4.65	*1.38*	3.12	3.90	*1.25*
Temperature	3.07	4.00	*1.30*	4.63	5.57	*1.20*
Cross sectional curvature	2.55	3.25	*1.27*	2.40	3.33	*1.39*
Slope	2.24	2.84	*1.27*	2.64	3.65	*1.38*
Vertical distance to channel network	2.00	2.62	*1.31*	2.78	3.74	*1.35*
Relative slope position	1.97	2.42	*1.23*	2.02	2.58	*1.28*
Catchment area	1.93	2.63	*1.36*	2.33	2.87	*1.23*
Convergence index	1.88	2.42	*1.29*	3.70	4.59	*1.24*
Topographic wetness index	1.85	2.60	*1.40*	1.60	2.09	*1.31*
RS predictors						
NDVI	7.11	–	n.a.[b]	2.45	–	n.a.
Landsat 1	1.98	–	n.a.	2.33	–	n.a.
Landsat 2	1.45	–	n.a.	1.45	–	n.a.
Landsat 3	1.80	–	n.a.	1.18	–	n.a.
Landsat 4	2.31	–	n.a.	2.73	–	n.a.
Landsat 5	1.91	–	n.a.	1.28	–	n.a.
Landsat 6	0.00	–	n.a.	3.93	–	n.a.
Landsat 7	1.57	–	n.a.	2.04	–	n.a.

[a] Remote sensing.
[b] Non-applicable.

the 1993 and 2008 maps and highlighting those pixel which SOC difference (as absolute value) was higher than the sum of the standard errors. In such pixels, SOC difference was considered as reliable.

3. Results

Distributions of observed and predicted data with and without remote sensing (RS) predictors were log shaped (Table 1 and Supplementary material Fig. 2). Distribution of predicted data showed similar skewness than observed data in 1993 and lower, but always positive, kurtosis in 1993 and kurtosis and skewness than observed data in 2008, which suggests that this method better estimates SOC in the central values of the distribution. All models had pseudo-R^2 higher than 0.693 for the 1993 model and 0.634 for 2008 model. Models with and without RS predictors had similar accuracy (Supplementary material Fig. 3). The removal of the RS predictors had a negligible effect on both the variation of the pseudo-R^2 and angular coefficient of the pseudo regression lines of both models, which was 0.43–0.45 in the 1993 and 0.33–0.34 in the 2008. Similarly, the intercepts were from 6.59 to 10.13 g organic C kg^{-1}, thus the predictions overestimated the observed value when SOC is low and down-estimated it when SOC is high.

Removal of the RS predictors slightly changed the ranking of the predictors in terms of contribution to the total variance explained (Table 2). Among the RS predictors, only NDVI in the 1993 model showed a relatively high contribution to the variability explained (7.11%, the 4th strongest predictor), whereas its importance was negligible in the 2008 model (2.45%, the 15th predictor).

In general, the removal of the RS predictors resulted in an increase of the contribution to the total variance of the lowest contributing predictors (Table 1), with the exception of rainfall (5.91% in the 1993 model and 4.21% in the 2008 model). Rainfall contribution to the total variance explained was 1.57 and 1.41 fold after removal of the RS predictors. In total, the removal of the RS predictors from the modelling procedure increased the total contribution to the total variance explained of the six most important non-RS predictors by 9.71% in 1993 and 8.08% in 2008. The most important predictor of SOC content in both the 1993 and 2008 models was texture (19.18% and 22.64%, respectively, in the models with RS predictors). The six most important non-RS predictors across all 4 models were soil texture, land use, valley depth, rainfall, channel network base level (that is correlated with the height above the see level [a.s.l.] of the basin upon each pixel and thus to the chance of receiving SOC by erosion) and LS factor.

In the models both with and without RS predictors, a discrepancy in the association between soil texture levels and relative importance for SOC prediction was found between the 1993 and 2008 models (Supplementary material Fig. 4). In the 1993 model, only Silty-Clay-Loam (texture 6) and Sandy-Loam (texture 7) showed a positive association to the SOC, whereas in the 2008 model, such a positive association was also found for Clay (texture 1), Sandy Clay Loam (texture 8), and Sandy soils (texture 9). In both models, CCP contributed more than VFO to SOC estimation and VFO more than ARA. Channel network base level negatively correlated with SOC estimation in the first half of its range in both the 1993 and 2008 models (up to 660 and 330 m a.s.l., respectively), after which its contribution to the function of SOC estimation was always positive and constant. Similar trends were observed for the rainfall to SOOC estimation relationship. The role played by valley depth was strong in the 1993 model, only. Valley depth, which is inversely correlated with the deposition process, positively associated with SOC only in the lowest SOC concentration samples.

As expected, the highest SOC concentrations were mostly found in sites with relatively low mean temperature and high rainfall, which, in this area, are conducive for C accumulation in soil (see Cannarozzo et al., 2006; and Viola et al., 2014 for maps of rainfall and temperatures). In our study area, these sites are mainly located at the boundaries of

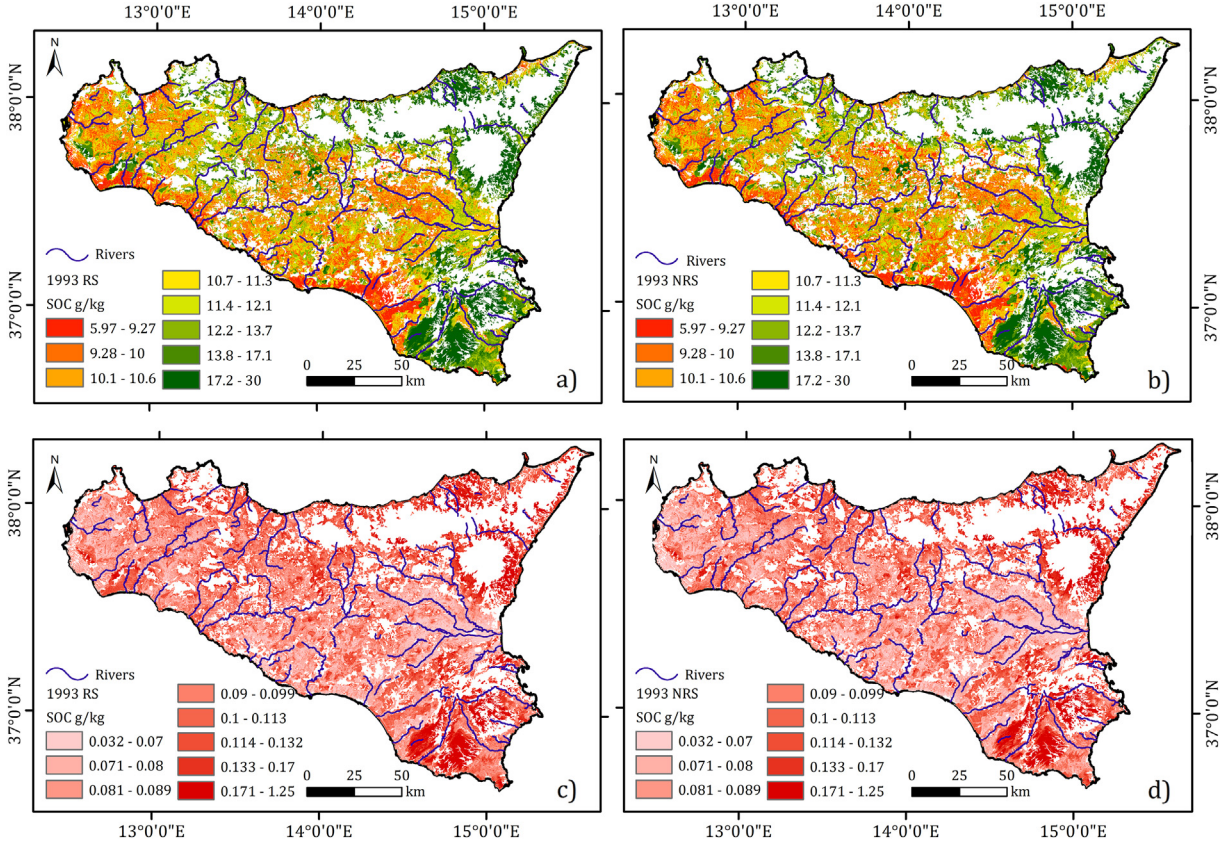

Fig. 2. One-hundred meters resolution maps of the SOC (expressed in g C kg^{-1}, a, b) and uncertainty maps (c, d) of the boosted regression trees models built with data from 1993 with (a, c) or without (b, d) remote sensed covariates. STD is for standard deviation. Please note that range vary among classes.

the mountain chains (Figs. 2 and 3): the northern mountain chains (Madonie, Nebrodi and Peloritani), the Volcano Etna in the eastern part of the island, the Sicani Mountains in the western part of the island, and to a certain extent the Hyblaean area in the south-eastern corner. In general, the higher the SOC concentration, the higher the standard error of the model. The models with RS showed a lower standard error than the models without RS, especially in 1993.

Classification of the predicted samples in the range ± 50% than the observed was high for both the 1993 and 2008 models (81% and 72% of the estimated data extracted on the same location of the entry data; Fig. 4) and well distributed in the area. Samples classified in the ranges < or >50% than the observed were also well distributed.

The removal of the RS predictors did not exert an effect on the SOC prediction, which was on average 11.9 g organic C kg^{-1} in ARA, 12.6 g organic C kg^{-1} in VFO, and 14.4 g organic C kg^{-1} in CCP (Fig. 5). Irrespective of the presence of the RS covariates in the model, such amount increased by 1.9%, 1.9% and 0.9% in ARA, VFO, and CCP, respectively, from 1993 to 2008 and such increase occurred in all land use groups considered in a similar extent (Supplementary material Fig. 5).

The variation of the SOC in the area under study strongly depended on the subarea within the region and did not match the SOC map at the baseline (1993) (Fig. 6) In contrast, the reliability of this difference [measured as $|SOC_{08-93}| - (STDEV_{08} + STDEV_{93})$] did not depend on the area and was positive in almost all pixels. An increase of SOC concentration (+10.1 g SOC kg^{-1} in the 99th percentile of the difference distribution, i.e. +0.67 g SOC kg^{-1} yr^{-1}, Supplementary material Fig. 6) was frequently found in the Hyblaean area, especially in the mountains and hilly environments, in the western hilly to plains areas, and, unexpectedly, on the central area located on the south of the northern mountain ridge. A loss of SOC (−6.6 g SOC kg^{-1} in the 1st percentile of the difference distribution, i.e. −0.44 g SOC kg^{-1} yr^{-1}) was observed in the areas surrounding the other mountains ridge, the areas between the eastern slope of Etna Volcano and the sea and the Catania plain to the south of Etna, the Hyblaean plains on the south of the Hyblaean Mountains, and in part of the far-western plains, near the western corner of the island.

4. Discussion

The understanding of the space-time variation of SOC is a prerequisite to hypothesize future scenarios and the outcome of any policy on crop yield, yield potential and ecosystem service (Dono et al., 2016; Elith et al., 2008; Luo et al., 2015; Novara et al., 2017). Thus SOC should be primarily managed to increase (agro)-ecosystem resilience to anthropic pressure and climate change. However, the mutual relationship of SOC and climate change depends on several variables (e.g. soil texture or tillage) and has wide variation (Kirschbaum, 1995; Stockmann et al., 2013). In this framework, the integration of short and long term comparisons (Conant et al., 2001; Kämpf et al., 2016; Kurganova et al., 2014; Post and Kwon, 2000) can strongly boost the accuracy of SOC prediction (Luo et al., 2015). However, single-point comparisons, even when analyzed for a wide timespan, have the drawback of being uncorrected for position in the stochastic population of the data and are thus not representative of wide areas.

In the present study, the integration of DSM and BRT modelling allowed us produce maps of probable agricultural topsoil SOC distribution (along with reliability and error maps) for two sampling campaigns performed 15 years apart (1993 and 2008). This also allowed us to estimate how SOC varied through space and time at each land use group (arables [ARA], tree-like crops [VFO], and cropped areas with semi-natural vegetation [CCP]) and the importance of some ecological characteristics on space-time SOC variation.

The study period was selected according to the highest availability of data within each campaign and its timespan (15 years) allowed us to

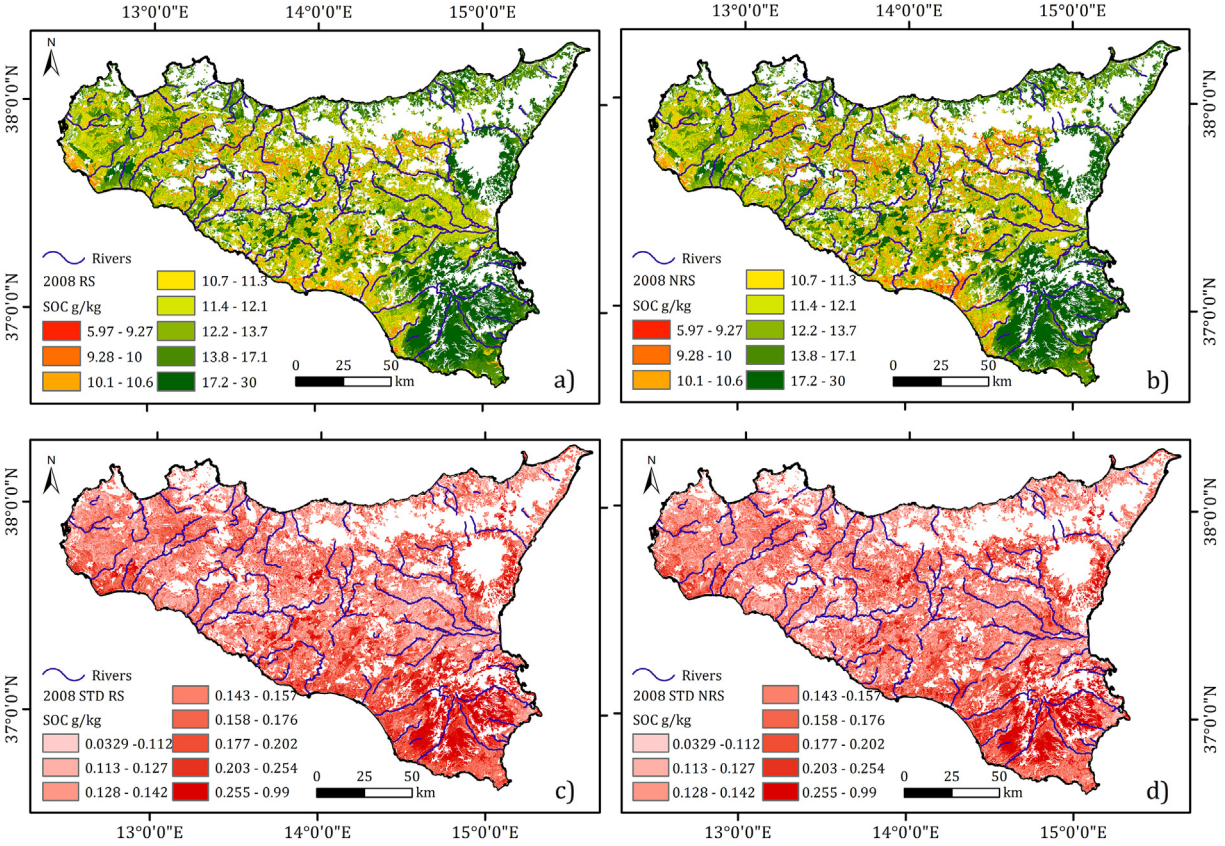

Fig. 3. One-hundred meters resolution maps of the SOC (expressed in g sC kg^{-1}, a, b) and uncertainty maps (c, d) of the boosted regression trees models built with data from 2008 with (a, c) or without (b, d) remote sensed covariates. STD is for standard deviation. Please note that range vary among classes.

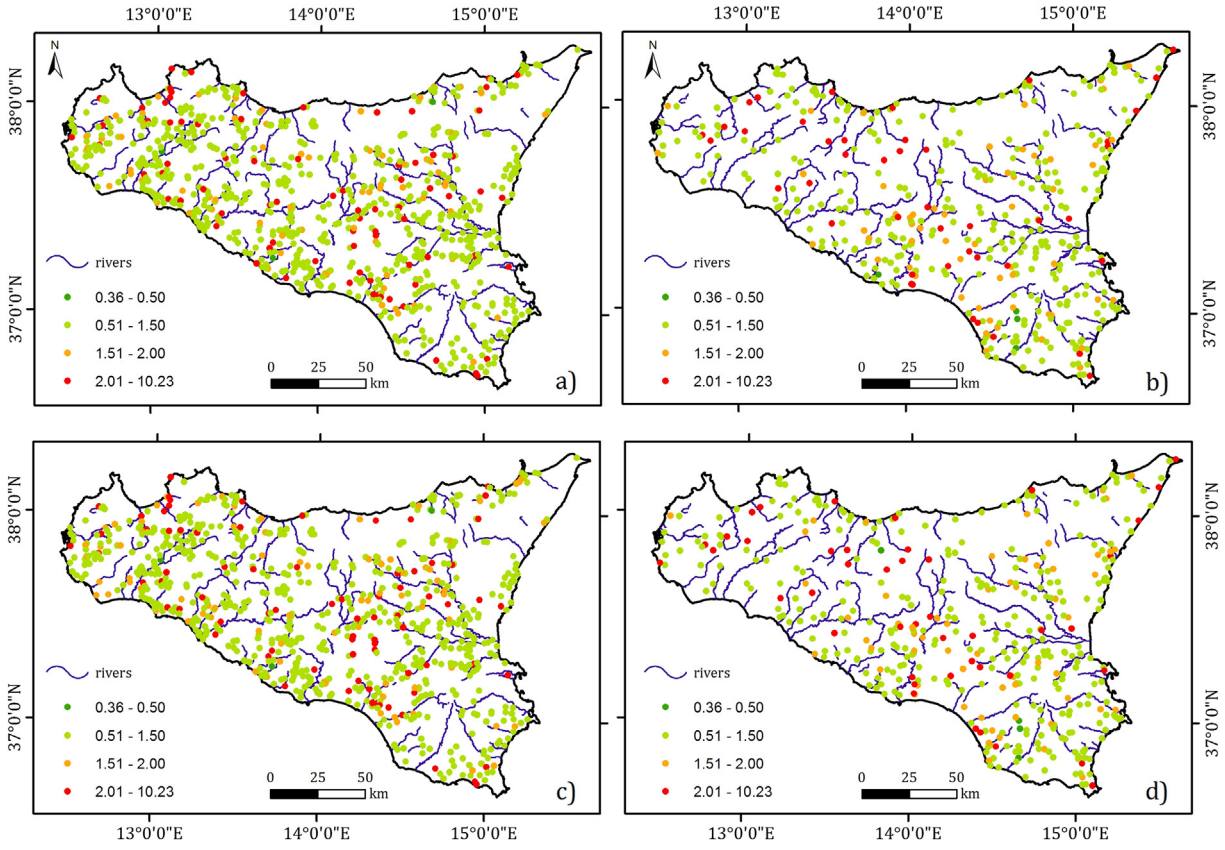

Fig. 4. Prediction confidence map of the boosted regression trees (BRT) models of 1993 (a, c) and 2008 (b, d) built with (a, b) or without (c, d) remote sensed predictors. Each point represents the ratio between BRT-predicted and observed values. The closer the ratio is to 1, the better its representation of the observed value is.

depict a short-term variation of SOC within a well-characterized period. Its beginning (1993) luckily fell soon before a number of European and worldwide policy measures which profoundly impacted agriculture, including the Regulation EEC 1272/88 on set-aside (compulsory from the 1992); the United Nations Framework Convention on Climate Change of 1993 (into force from 1994); and the World Trade Organization Marrakesh Agreement of 1994. Similarly, its end (2008 campaign) fell soon after the abolishment of the compulsory set-aside in the EU (Common Agricultural Policy [CAP] health check 2008) and the decoupled CAP EU payments to agriculture in 2005 (Regulation EEC 1782/2003). This collocates our research study in a period of low agricultural dynamic in term of land use change and management techniques, the latter of which were dominated by durum wheat continuous cultivation (in ARA) and deep plowing.

Indeed, we found that the area covered by ARA and that by VFO were almost constant during the study period (1993 to 2008), whereas the area covered by CCP increased by 55%, which was likely due to the temporarily conversion of grassland to pastures. As expected, we found that SOC of ARA was predicted as lower than VFO and that of VFO lower than CCP. The increase in the SOC stock during the study period was however partly unexpected. From the one hand, we expected to find an increase in the ARA and VFO due to many conditions. These include the application of Good Agricultural and Environmental Conditions (Borrelli et al., 2016), which effects on ARA were directly elucidated in similar environments (Ventrella et al., 2011); the high clay content in the soils cropped with these species, as directly addressed by Zinn et al. (2005a, 2005b); massive recourse to the set-aside (partly compulsory); the minor role of climate change in agricultural areas (Cannarozzo et al., 2006; Fantappiè et al., 2011); and ease of SOC increase in low-SOC soils (Kämpf et al., 2016), such as those in the present study (<12.6 g kg^{-1} ± 0.21 g kg^{-1}). From the other hand, such an increase was expected to occur in the northern, rainy, part of Sicily thanks to the presence of conditions conducive to a SOC accumulation, rather than in the southern, more arid parts, whereas we found an opposite pattern. Nonetheless, these results agree with those of other lower resolution studies in the same area (Chiti et al., 2012; Fantappiè et al., 2011; Freibauer et al., 2004; Hashimoto et al., 2016; Lugato et al., 2014) or studies conducted in similar environments (Farina et al., 2016; Rodríguez Martín et al., 2016), where soil management exerted an important role in the percentage or reduction of SOC in relatively humid areas.

Climate change effect on Sicily is under debate: no change in the rainfall in most of ARA and VFO-dominated areas is expected

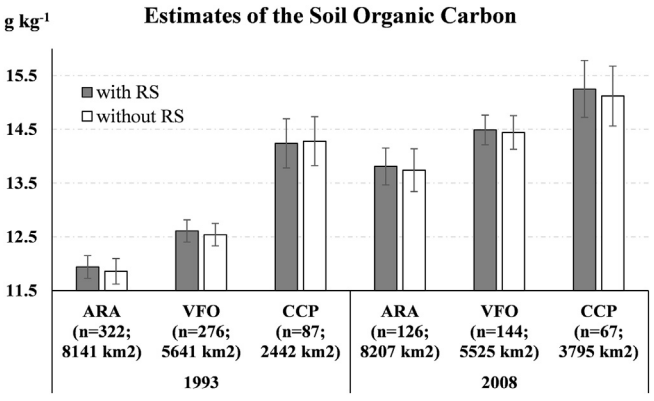

Fig. 5. Estimates of the soil organic carbon in each of the land use groups used in the present study as affected by the presence of the remote sensed (RS) covariates in the model. ARA is for non-irrigated arable land; VFO is for vineyards, fruit trees and berry plantations, and olive groves; CCP is for annual crops associated with permanent crops, complex cultivation patterns, land principally occupied by agriculture, with significant areas of natural vegetation. Data are means ± standard error. Number of sampling points falling into an area of each land use group is shown.

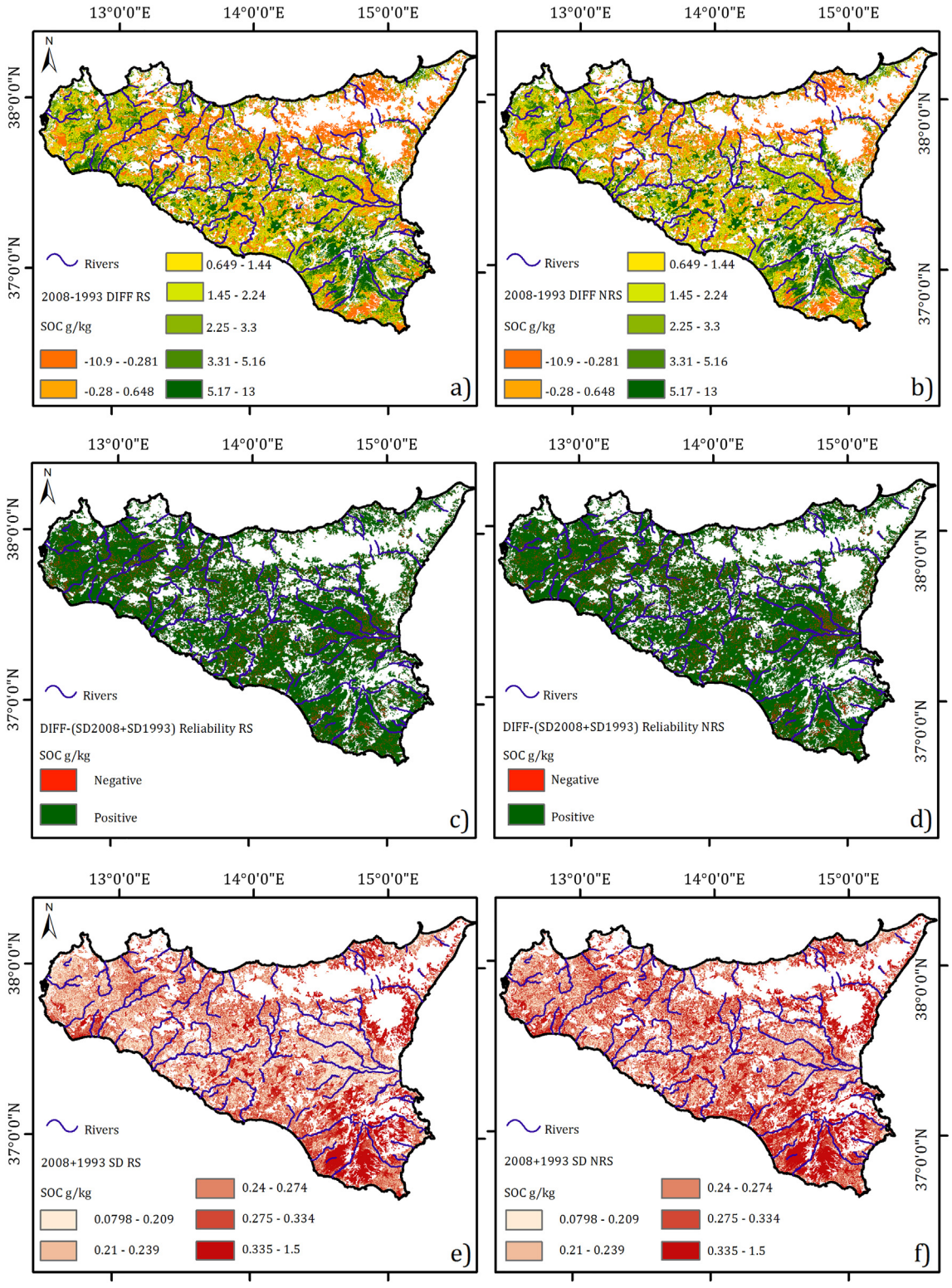

Fig. 6. One-hundred meters resolution map of the difference in the SOC (expressed in g C kg^{-1}) during the study period (a, b). Reddish pixels in a and b panels indicate a loss and greenish pixels a gain in the SOC in 2008 compared to 1993. Please note that range vary among classes. Reliability (c, d) of the maps in a and b panels, respectively, computed as the difference between the SOC difference (SOC_{08}–SOC_{93}, in absolute value) and the sum of the standard errors (in lower panels of Figs. 2 and 3). Green points indicate those pixels in which the difference of SOC is reliable (i.e. reliability is higher than 0). Maps of the sum of the standard deviations of the 'map of SOC' (e, f). SD is for sum of standard deviations. Each computation and mapping was made for models built with (a, c, and e) and without (b, d, and f) remote sensing (RS) predictors. (For interpretation of the references to colour in this figure legend, the reader is referred to the web version of this article.)

(Cannarozzo et al., 2006), and a temperature increase is likely to occur (Viola et al., 2014). However, the interaction between water availability and temperature with the effect of soil traits and land use on potential and actual mineralization and C inputs are yet to be clarified (Badagliacca et al., 2017; Bogunović et al., 2017b; Davidson and Janssens, 2006; Purton et al., 2015). For example, in a high organic C

area (Galapagos), Rial et al. (2017) suggested that the increase in the amount of rainfall and, in general, water availability (through occult precipitations, too) will likely consist in an increase of the SOC stock.

During this 15-years study (1993–2008), mean increase in SOC in the agricultural area of the region (median = +1.62 g C kg^{-1} soil; lower confidence interval 95%: −4.86 g C kg^{-1}; upper confidence interval 95%: +8.40 g C kg^{-1}) appeared similar to the time trends in temperature and rainfall observed in the region (Cannarozzo et al., 2006; Viola et al., 2014) and the degree of lithological and soil diversity (Costantini and L'Abate, 2016; Fantappiè et al., 2015). This occurred despite the most important predictors of SOC at any pixel were soil texture, land use and topographic covariates, as also found elsewhere (Bogunović et al., 2017b), whereas rainfall and temperature only contributed by 8.98% and 8.94% of the total variability explained in the 1993 and 2008 model, respectively. Grinand et al. (2017), by means of an algorithm similar to the one we used, found that SOC change modelled in a 20-years timespan was likely negative in humid and not different than zero in arid areas and that such variation strongly depended on both the climatic predictors and degree of deforestation. However, in contrast to Grinand et al. (2017), we found an increase of the CCP, which effect on SOC is more similar to that of forests compared to ARA and VFO.

A matching between SOC and climatic gradient was observed by Vaysse and Lagacherie (2015) in southern France, a colder and more rainy environment than Sicily. In addition, in the 'Vaysse and Lagacherie (2015)' modelling of soil traits, a similarity among maps of SOC, soil pH and soil clay content can be observed. It is likely that in our environment, the variability of some important traits related to soil erosion and deposition (such as valley depth and channel network base level) and thus C movements by erosion and deposition across pixel was better related to trends in rainfall and temperature, than their long-term mean. Nevertheless, the present results only partly fitted the erosion risk map published soon before the beginning (Ferro et al., 1991) or the end (Fantappiè et al., 2015) of the present experiment. This latter discrepancy can depend on both the difference in the spatial resolution between the present map and those of Ferro et al. (1991) and Fantappiè et al. (2015) and the lack in these of the information about the deposition of the eroded soil and C (Adhikari et al., 2014). Indeed, we found that catchment area, landforms, valley depth and channel network base level, which are related to soil deposition, contributed by 20.3% and 18.2% of the total SOC variability explained in 1993 and 2008, respectively. Topographic indices can strongly affect SOC concentration through erosion and deposition, whereas their role in SOC stock can be minimal (Grimm et al., 2008; Schillaci et al., 2017). In the present work, we found that RS indices minimally increased the pseudo-R^2 of the fitting functions and mostly affected both the variance explained by each covariate and the variability among model replicates. In particular, the RS covariates captured on their whole 18.1% and 17.4% of the total variance explained in the 1993 and 2008, respectively. Bou Kheir et al. (2010) found that removal of RS indices can increase the total variance explained by the less important predictors and, in contrast to the present study, also the overall accuracy of the model. Other studies indicated that the importance of RS indices in SOC mapping can depend on a range of factors, including the variable mapped, the resolution of the measured and ancillary variables, the extent of the study and the importance of the processes of SOC accumulation in relation to the study area (Castaldi et al., 2016b; Grinand et al., 2017; Poggio et al., 2013; Priori et al., 2016). It is thus likely that the high number of non-RS covariates in this work and their ability to explain a high degree of variability reduced the ability of the RS data to explain an additional amount of variability. In addition, the need of using more than one Landsat image (each of which took 13–32 days apart from each other) could have reduced the importance of RS indices for the whole area and impaired their contribution to the prediction. Similarly, some experiments with fewer input points and or coarser covariates than the present found a high percentage of variance explained by the RS indices in either SOC or other environmental traits (Akpa et al., 2016; Castaldi et al., 2016b; Wang et al., 2016).

5. Conclusions

In the present work, two legacy sub-datasets of SOC concentration were integrated in a DSM procedure to estimate the SOC variation along a 15-years period (1993–2008). This result was possible since the application of the covariates produced a pseudo-R^2 of SOC representation of 0.63–0.69, which allowed a time comparison of SOC at the pixel level. Texture and land use classes showed the highest predictor importance, around one third of the variance explained. Yigini and Panagos (2016) indicated these traits as capable of having a short-term impact on the SOC higher than climate-driven processes.

The integration of RS indices used in this study did not increase the pseudo-R^2, but captured about one fifth of the total variance explained by the covariates and strongly reduced the modelling variability. This suggests that their integration in the models can overcome problems related to erroneous attribution of some samples to the other covariate levels.

Finally, the present results can imply both agronomic and policy consequences at the district level and call for an intervention on soil fertility to maintain agriculture productivity (Dono et al., 2016). These results can help in calibrating models of SOC dynamic under various management or climate change scenarios, especially at regional extent, by removing the noise in the modelling phase by a correction with RS or other soil traits and geographical covariates, as already shown with other disturbing covariates in SOC modelling (Bogunović et al., 2017a, 2017b; Zinn et al., 2005b), which provide measures of covariates with a unique resolution in broad areas.

Acknowledgment

The authors are grateful to Maria Gabriella Matranga, Vito Ferraro and Fabio Guaitoli from the Regional Bureau for Agriculture, rural Development and Mediterranean Fishery, the Department of Agriculture, Service 7 UOS7.03 Geographical Information Systems, Cartography and Broadband Connection in Agriculture, Palermo. The authors also thank three anonymous reviewers for their constructive comments, which helped to improve the manuscript.

Appendix A. Supplementary data

Supplementary data to this article can be found online at http://dx.doi.org/10.1016/j.scitotenv.2017.05.239.

References

Adhikari, K., Hartemink, A.E., Minasny, B., Bou Kheir, R., Greve, M.B., Greve, M.H., 2014. Digital mapping of soil organic carbon contents and stocks in Denmark. PLoS One 9, e105519. http://dx.doi.org/10.1371/journal.pone.0105519.

Akpa, S.I.C., Odeh, I.O.A., Bishop, T.F.A., Hartemink, A.E., Amapu, I.Y., 2016. Total soil organic carbon and carbon sequestration potential in Nigeria. Geoderma 271:202–215. http://dx.doi.org/10.1016/j.geoderma.2016.02.021.

Badagliacca, G., Ruisi, P., Rees, R.M., Saia, S., 2017. An assessment of factors controlling N_2O and CO_2 emissions from crop residues using different measurement approaches. Biol. Fertil. Soils http://dx.doi.org/10.1007/s00374-017-1195-z.

Bogunović, I., Pereira, P., Brevik, E.C., 2017a. Spatial distribution of soil chemical properties in an organic farm in Croatia. Sci. Total Environ. 584–585:535–545. http://dx.doi.org/10.1016/j.scitotenv.2017.01.062.

Bogunović, I., Trevisani, S., Šeput, M., Juzbašić, D., Đurđević, B., 2017b. Short-range and regional spatial variability of soil chemical properties in an agro-ecosystem in eastern Croatia. Catena (Cremlingen) 156, 1–11.

Borrelli, P., Paustian, K., Panagos, P., Jones, A., Schütt, B., Lugato, E., 2016. Effect of good agricultural and environmental conditions on erosion and soil organic carbon balance: a national case study. Land Use Policy 50:408–421. http://dx.doi.org/10.1016/j.landusepol.2015.09.033.

Bou Kheir, R., Greve, M.H., Bøcher, P.K., Greve, M.B., Larsen, R., McCloy, K., 2010. Predictive mapping of soil organic carbon in wet cultivated lands using classification-tree based models: the case study of Denmark. J. Environ. Manag. 91:1150–1160. http://dx.doi.org/10.1016/j.jenvman.2010.01.001.

Bradford, M.A., Wieder, W.R., Bonan, G.B., Fierer, N., Raymond, P.A., Crowther, T.W., 2016. Managing uncertainty in soil carbon feedbacks to climate change. Nat. Clim. Chang. 6: 751–758. http://dx.doi.org/10.1038/nclimate3071.

Bruun, T.B., Elberling, B., de Neergaard, A., Magid, J., 2015. Organic carbon dynamics in different soil types after conversion of forest to agriculture. L. Degrad. Dev. 26:272–283. http://dx.doi.org/10.1002/ldr.2205.

Bui, E., Henderson, B., Viergever, K., 2009. Using knowledge discovery with data mining from the Australian Soil Resource Information System database to inform soil carbon mapping in Australia. Global Biogeochem. Cycles 23 (doi:Artn Gb4033\rDoi 10.1029/2009gb003506).

Cannarozzo, M., Noto, L.V., Viola, F., 2006. Spatial distribution of rainfall trends in Sicily (1921–2000). Phys. Chem. Earth, Parts A/B/C 31:1201–1211. http://dx.doi.org/10.1016/j.pce.2006.03.022.

Castaldi, F., Castrignanò, A., Casa, R., 2016a. A data fusion and spatial data analysis approach for the estimation of wheat grain nitrogen uptake from satellite data. Int. J. Remote Sens. 37:4317–4336. http://dx.doi.org/10.1080/01431161.2016.1212423.

Castaldi, F., Palombo, A., Santini, F., Pascucci, S., Pignatti, S., Casa, R., 2016b. Evaluation of the potential of the current and forthcoming multispectral and hyperspectral imagers to estimate soil texture and organic carbon. Remote Sens. Environ. 179:54–65. http://dx.doi.org/10.1016/j.rse.2016.03.025.

Chartin, C., Stevens, A., Goidts, E., Krüger, I., Carnol, M., van Wesemael, B., 2017. Mapping Soil Organic Carbon stocks and estimating uncertainties at the regional scale following a legacy sampling strategy (Southern Belgium, Wallonia). Geoderma Reg. 9: 73–86. http://dx.doi.org/10.1016/j.geodrs.2016.12.006.

Chiti, T., Gardin, L., Perugini, L., Quaratino, R., Vaccari, F.P., Miglietta, F., Valentini, R., 2012. Soil organic carbon stock assessment for the different cropland land uses in Italy. Biol. Fertil. Soils 48:9–17. http://dx.doi.org/10.1007/s00374-011-0599-4.

Conant, R.T., Paustian, K., Elliott, E.T., 2001. Grassland management and conversion into grassland: effects on soil carbon. Ecol. Appl. 11:343–355. http://dx.doi.org/10.1890/1051-0761(2001)011[0343:GMACIG]2.0.CO;2.

Conant, R.T., Ogle, S.M., Paul, E.A., Paustian, K., 2011. Measuring and monitoring soil organic carbon stocks in agricultural lands for climate mitigation. Front. Ecol. Environ. 9:169–173. http://dx.doi.org/10.1890/090153.

Conrad, O., Bechtel, B., Bock, M., Dietrich, H., Fischer, E., Gerlitz, L., Wehberg, J., Wichmann, V., Böhner, J., 2015. System for Automated Geoscientific Analyses (SAGA) v. 2.1.4. Geosci. Model Dev. 8:1991–2007. http://dx.doi.org/10.5194/gmd-8-1991-2015.

Costantini, E.A.C., L'Abate, G., 2016. Beyond the concept of dominant soil: preserving pedodiversity in upscaling soil maps. Geoderma 271:243–253. http://dx.doi.org/10.1016/j.geoderma.2015.11.024.

Davidson, E.A., Janssens, I.A., 2006. Temperature sensitivity of soil carbon decomposition and feedbacks to climate change. Nature 440:165–173. http://dx.doi.org/10.1038/nature04514.

Doetterl, S., Stevens, A., Six, J., Merckx, R., Van Oost, K., Casanova Pinto, M., Casanova-Katny, A., Muñoz, C., Boudin, M., Zagal Venegas, E., Boeckx, P., 2015. Soil carbon storage controlled by interactions between geochemistry and climate. Nat. Geosci. 8: 780–783. http://dx.doi.org/10.1038/ngeo2516.

Dono, G., Cortignani, R., Dell'Unto, D., Deligios, P., Doro, L., Lacetera, N., Mula, L., Pasqui, M., Quaresima, S., Vitali, A., Roggero, P.P., 2016. Winners and losers from climate change in agriculture: insights from a case study in the Mediterranean basin. Agric. Syst. 147: 65–75. http://dx.doi.org/10.1016/j.agsy.2016.05.013.

Elith, J., Leathwick, J.R., Hastie, T., 2008. A working guide to boosted regression trees. J. Anim. Ecol. http://dx.doi.org/10.1111/j.1365-2656.2008.01390.x.

Fantappiè, M., L'Abate, G., Costantini, E.A.C., 2011. The influence of climate change on the soil organic carbon content in Italy from 1961 to 2008. Geomorphology 135:343–352. http://dx.doi.org/10.1016/j.geomorph.2011.02.006.

Fantappiè, M., Priori, S., Costantini, E.A.C., 2015. Soil erosion risk, Sicilian Region (1:250,000 scale). J. Maps 11:323–341. http://dx.doi.org/10.1080/17445647.2014.956349.

Farina, R., Marchetti, A., Francaviglia, R., Napoli, R., Bene, C. Di, 2016. Modeling regional soil C stocks and CO_2 emissions under Mediterranean cropping systems and soil types. Agric. Ecosyst. Environ. http://dx.doi.org/10.1016/j.agee.2016.08.015.

Ferro, V., Giordano, G., Iovino, M., 1991. Isoerosivity and erosion risk map for Sicily. Hydrol. Sci. J. 36:549–564. http://dx.doi.org/10.1080/02626669109492543.

Filippi, P., Minasny, B., Cattle, S.R., Bishop, T.F.A., 2016. Chapter Four – Monitoring and Modeling Soil Change: The Influence of Human Activity and Climatic Shifts on Aspects of Soil Spatiotemporally. Advances in Agronomy:pp. 153–214 http://dx.doi.org/10.1016/bs.agron.2016.06.001.

Forkuor, G., Hounkpatin, O.K.L., Welp, G., Thiel, M., Zhu, A.-X., Scholten, T., Koch, B., Shepherd, K., 2017. High resolution mapping of soil properties using remote sensing variables in South-Western Burkina Faso: a comparison of machine learning and multiple linear regression models. PLoS One 12, e0170478. http://dx.doi.org/10.1371/journal.pone.0170478.

Francaviglia, R., Renzi, G., Ledda, L., Benedetti, A., 2017. Organic carbon pools and soil biological fertility are affected by land use intensity in Mediterranean ecosystems of Sardinia, Italy. Sci. Total Environ. 599–600:789–796. http://dx.doi.org/10.1016/j.scitotenv.2017.05.021.

Freibauer, A., Rounsevell, M.D., Smith, P., Verhagen, J., 2004. Carbon sequestration in the agricultural soils of Europe. Geoderma 122:1–23. http://dx.doi.org/10.1016/j.geoderma.2004.01.021.

Freund, Y., Schapire, R.E., 1997. A decision-theoretic generalization of on-line learning and an application to boosting. J. Comput. Syst. Sci. 55:119–139. http://dx.doi.org/10.1006/jcss.1997.1504.

Gasch, C.K., Gräler, B., Meyer, H., Magney, T.S., Brown, D.J., 2015. Spatio-temporal interpolation of soil water, temperature, and electrical conductivity in 3D + T: the Cook Agronomy Farm data set. Spat. Stat. 14:70–90. http://dx.doi.org/10.1016/j.spasta.2015.04.001.

Grimm, R., Behrens, T., Märker, M., Elsenbeer, H., 2008. Soil organic carbon concentrations and stocks on Barro Colorado Island - digital soil mapping using Random Forests analysis. Geoderma 146:102–113. http://dx.doi.org/10.1016/j.geoderma.2008.05.008.

Grinand, C., Maire, G. Le, Vieilledent, G., Razakamanarivo, H., Razafimbelo, T., Bernoux, M., 2017. Estimating temporal changes in soil carbon stocks at ecoregional scale in Madagascar using remote-sensing. Int. J. Appl. Earth Obs. Geoinf. 54:1–14. http://dx.doi.org/10.1016/j.jag.2016.09.002.

de Gruijter, J.J., McBratney, A.B., Minasny, B., Wheeler, I., Malone, B.P., Stockmann, U., 2016. Farm-scale soil carbon auditing. Geoderma 265:120–130. http://dx.doi.org/10.1016/j.geoderma.2015.11.010.

Guyot, G., Gu, X.-F., 1994. Effect of radiometric corrections on NDVI-determined from SPOT-HRV and Landsat-TM data. Remote Sens. Environ. 49:169–180. http://dx.doi.org/10.1016/0034-4257(94)90012-4.

Hashimoto, S., Nanko, K., Ťupek, B., Lehtonen, A., 2016. Data-mining analysis of factors affecting the global distribution of soil carbon in observational databases and Earth system models. Geosci. Model Dev. Discuss.:1–22 http://dx.doi.org/10.5194/gmd-2016-138.

Henderson, B.L., Bui, E.N., Moran, C.J., Simon, D.A.P., 2005. Australia-wide predictions of soil properties using decision trees. Geoderma 124:383–398. http://dx.doi.org/10.1016/j.geoderma.2004.06.007.

Hengl, T., de Jesus, J.M., MacMillan, R.A., Batjes, N.H., Heuvelink, G.B.M., Ribeiro, E., Samuel-Rosa, A., Kempen, B., Leenaars, J.G.B., Walsh, M.G., Gonzalez, M.R., 2014. SoilGrids1km — global soil information based on automated mapping. PLoS One 9, e105992. http://dx.doi.org/10.1371/journal.pone.0105992.

Hengl, T., Mendes de Jesus, J., Heuvelink, G.B.M., Ruiperez Gonzalez, M., Kilibarda, M., Blagotić, A., Shangguan, W., Wright, M.N., Geng, X., Bauer-Marschallinger, B., Guevara, M.A., Vargas, R., MacMillan, R.A., Batjes, N.H., Leenaars, J.G.B., Ribeiro, E., Wheeler, I., Mantel, S., Kempen, B., 2017. SoilGrids250m: global gridded soil information based on machine learning. PLoS One 12, e0169748. http://dx.doi.org/10.1371/journal.pone.0169748.

Hijmans, R.J., Cameron, S.E., Parra, J.L., Jones, P.G., Jarvis, A., 2005. Very high resolution interpolated climate surfaces for global land areas. Int. J. Climatol. 25:1965–1978. http://dx.doi.org/10.1002/joc.1276.

Kämpf, I., Hölzel, N., Störrle, M., Broll, G., Kiehl, K., 2016. Potential of temperate agricultural soils for carbon sequestration: a meta-analysis of land-use effects. Sci. Total Environ. 566–567:428–435. http://dx.doi.org/10.1016/j.scitotenv.2016.05.067.

Kirschbaum, M.U.F., 1995. The temperature dependence of soil organic matter decomposition, and the effect of global warming on soil organic C storage. Soil Biol. Biochem. 27:753–760. http://dx.doi.org/10.1016/0038-0717(94)00242-S.

Kurganova, I., Lopes de Gerenyu, V., Six, J., Kuzyakov, Y., 2014. Carbon cost of collective farming collapse in Russia. Glob. Chang. Biol. 20:938–947. http://dx.doi.org/10.1111/gcb.12379.

Lacoste, M., Minasny, B., McBratney, A., Michot, D., Viaud, V., Walter, C., 2014. High resolution 3D mapping of soil organic carbon in a heterogeneous agricultural landscape. Geoderma 213:296–311. http://dx.doi.org/10.1016/j.geoderma.2013.07.002.

Legendre, P., Legendre, L., 1998. Numerical ecology. Developments in Environmental Modelling, Second English ed. http://dx.doi.org/10.1017/CBO9781107415324.004.

Lombardo, L., Cama, M., Conoscenti, C., Märker, M., Rotigliano, E., 2015. Binary logistic regression versus stochastic gradient boosted decision trees in assessing landslide susceptibility for multiple-occurring landslide events: application to the 2009 storm event in Messina (Sicily, southern Italy). Nat. Hazards 79:1621–1648. http://dx.doi.org/10.1007/s11069-015-1915-3.

Lugato, E., Bampa, F., Panagos, P., Montanarella, L., Jones, A., 2014. Potential carbon sequestration of European arable soils estimated by modelling a comprehensive set of management practices. Glob. Chang. Biol. 20:3557–3567. http://dx.doi.org/10.1111/gcb.12551.

Luo, Z., Wang, E., Zheng, H., Baldock, J.A., Sun, O.J., Shao, Q., 2015. Convergent modelling of past soil organic carbon stocks but divergent projections. Biogeosciences 12: 4373–4383. http://dx.doi.org/10.5194/bg-12-4373-2015.

Maia, S.M.F., Ogle, S.M., Cerri, C.E.P., Cerri, C.C., 2010. Soil organic carbon stock change due to land use activity along the agricultural frontier of the southwestern Amazon, Brazil, between 1970 and 2002. Glob. Chang. Biol. 16:2775–2788. http://dx.doi.org/10.1111/j.1365-2486.2009.02105.x.

Martin, M.P., Wattenbach, M., Smith, P., Meersmans, J., Jolivet, C., Boulonne, L., Arrouays, D., 2011. Spatial distribution of soil organic carbon stocks in France. Biogeosciences 8:1053–1065. http://dx.doi.org/10.5194/bg-8-1053-2011.

Martin, M.P., Orton, T.G., Lacarce, E., Meersmans, J., Saby, N.P.A., Paroissien, J.B., Jolivet, C., Boulonne, L., Arrouays, D., 2014. Evaluation of modelling approaches for predicting the spatial distribution of soil organic carbon stocks at the national scale. Geoderma 223–225:97–107. http://dx.doi.org/10.1016/j.geoderma.2014.01.005.

Meersmans, J., De Ridder, F., Canters, F., De Baets, S., Van Molle, M., 2008. A multiple regression approach to assess the spatial distribution of Soil Organic Carbon (SOC) at the regional scale (Flanders, Belgium). Geoderma 143:1–13. http://dx.doi.org/10.1016/j.geoderma.2007.08.025.

Meersmans, J., Van Wesemael, B., Van Molle, M., 2009. Determining soil organic carbon for agricultural soils: a comparison between the Walkley & Black and the dry combustion methods (north Belgium). Soil Use Manag. 25:346–353. http://dx.doi.org/10.1111/j.1475-2743.2009.00242.x.

Miller, B.A., Koszinski, S., Wehrhan, M., Sommer, M., 2015a. Impact of multi-scale predictor selection for modeling soil properties. Geoderma 239:97–106. http://dx.doi.org/10.1016/j.geoderma.2014.09.018.

Miller, B.A., Koszinski, S., Wehrhan, M., Sommer, M., 2015b. Comparison of spatial association approaches for landscape mapping of soil organic carbon stocks. Soil 1: 217–233. http://dx.doi.org/10.5194/soil-1-217-2015.

Miller, B.A., Koszinski, S., Hierold, W., Rogasik, H., Schröder, B., Van Oost, K., Wehrhan, M., Sommer, M., 2016. Towards mapping soil carbon landscapes: issues of sampling scale

and transferability. Soil Tillage Res. 156:194–208. http://dx.doi.org/10.1016/j.still.2015.07.004.
Minasny, B., McBratney, A.B., Malone, B.P., Wheeler, I., 2013. Digital mapping of soil carbon. Adv. Agron. 118:1–47. http://dx.doi.org/10.1016/B978-0-12-405942-9.00001-3.
Novara, A., Gristina, L., Kuzyakov, Y., Schillaci, C., Laudicina, V.A., La Mantia, T., 2013. Turnover and availability of soil organic carbon under different Mediterranean land-uses as estimated by 13 C natural abundance. Eur. J. Soil Sci. 64:466–475. http://dx.doi.org/10.1111/ejss.12038.
Novara, A., Gristina, L., Sala, G., Galati, A., Crescimanno, M., Cerdà, A., Badalamenti, E., La Mantia, T., 2017. Agricultural land abandonment in Mediterranean environment provides ecosystem services via soil carbon sequestration. Sci. Total Environ. 576: 420–429. http://dx.doi.org/10.1016/j.scitotenv.2016.10.123.
Ogle, S.M., Breidt, F.J., Easter, M., Williams, S., Killian, K., Paustian, K., 2010. Scale and uncertainty in modeled soil organic carbon stock changes for US croplands using a process-based model. Glob. Chang. Biol. 16:810–822. http://dx.doi.org/10.1111/j.1365-2486.2009.01951.x.
Orton, T.G., Pringle, M.J., Page, K.L., Dalal, R.C., Bishop, T.F.A., 2014. Spatial prediction of soil organic carbon stock using a linear model of coregionalisation. Geoderma 230: 119–130. http://dx.doi.org/10.1016/j.geoderma.2014.04.016.
Paolanti, M., Costantini, E.A.C., Fantappiè, M., Barbetti, R., 2010. La descrizione del suolo. In: Costantini, E.A.C. (Ed.), Linee Guida Dei Metodi per Il Rilevamento E L'informatizzazione Dei Dati Pedologici. SELCA, Firenze, Italia.
Parras-Alcántara, L., Lozano-García, B., Keesstra, S., Cerdà, A., Brevik, E.C., 2016. Long-term effects of soil management on ecosystem services and soil loss estimation in olive grove top soils. Sci. Total Environ. 571:498–506. http://dx.doi.org/10.1016/j.scitotenv.2016.07.016.
Poggio, L., Gimona, A., Brewer, M.J., 2013. Regional scale mapping of soil properties and their uncertainty with a large number of satellite-derived covariates. Geoderma 209:1–14. http://dx.doi.org/10.1016/j.geoderma.2013.05.029.
Post, W.M., Kwon, K.C., 2000. Soil carbon sequestration and land-use change: processes and potential. Glob. Chang. Biol. 6:317–327. http://dx.doi.org/10.1046/j.1365-2486.2000.00308.x.
Priori, S., Fantappiè, M., Bianconi, N., Ferrigno, G., Pellegrini, S., Costantini, E.A.C., 2016. Field-scale mapping of soil carbon stock with limited sampling by coupling gamma-ray and Vis-NIR spectroscopy. Soil Sci. Soc. Am. J. 80:954. http://dx.doi.org/10.2136/sssaj2016.01.0018.
Purton, K., Pennock, D., Leinweber, P., Walley, F., 2015. Will changes in climate and land use affect soil organic matter composition? Evidence from an ecotonal climosequence. Geoderma 253–254:48–60. http://dx.doi.org/10.1016/j.geoderma.2015.04.007.
R_Development_Core_Team, 2008. R: A Language and Environment for Statistical Computing. Vienna Austria R Found. Stat. Comput http://dx.doi.org/10.1007/978-3-540-74686-7.
Rial, M., Martínez Cortizas, A., Taboada, T., Rodríguez-Lado, L., 2017. Soil organic carbon stocks in Santa Cruz Island, Galapagos, under different climate change scenarios. Catena 156:74–81. http://dx.doi.org/10.1016/j.catena.2017.03.020.
Rodríguez Martín, J.A., Álvaro-Fuentes, J., Gonzalo, J., Gil, C., Ramos-Miras, J.J., Grau Corbí, J.M., Boluda, R., 2016. Assessment of the soil organic carbon stock in Spain. Geoderma 264:117–125. http://dx.doi.org/10.1016/j.geoderma.2015.10.010.
Ross, C.W., Grunwald, S., Myers, D.B., 2013. Spatiotemporal modeling of soil organic carbon stocks across a subtropical region. Sci. Total Environ. 461–462:149–157. http://dx.doi.org/10.1016/j.scitotenv.2013.04.070.
Rouse Jr., J., Haas, R., Schell, J., Deering, D., 1974. Monitoring vegetation systems in the Great Plains with ERTS. In: Fraden, S., Marcanti, E., Becker, M. (Eds.), Third ERTS-1 Symposium. NASA-SP-351, Washington DC, pp. 309–317.
Ruisi, P., Giambalvo, D., Saia, S., Di Miceli, G., Frenda, A.S.A.S., Plaia, A., Amato, G., 2014. Conservation tillage in a semiarid Mediterranean environment: results of 20 years of research. Ital. J. Agron. 9:1. http://dx.doi.org/10.4081/ija.2014.560.
Saia, S., Benítez, E., García-Garrido, J.M., Settanni, L., Amato, G., Giambalvo, D., 2014. The effect of arbuscular mycorrhizal fungi on total plant nitrogen uptake and nitrogen recovery from soil organic material. J. Agric. Sci. 152:370–378. http://dx.doi.org/10.1017/S002185961300004X.
Schillaci, C., Braun, A., Kropácek, J., 2015. Terrain analysis and landform recognition. In: Clarke, L.E., Nield, J.M. (Eds.), Geomorphological Techniques (Online Edition). Chapter 2.4.2. British Society for Geomorphology, London, UK (ISSN: 2047-0371. p. 2.4.2).
Schillaci, C., Lombardo, L., Saia, S., Fantappiè, M., Märker, M., Acutis, M., 2017. Modelling the topsoil carbon stock of agricultural lands with the Stochastic Gradient Treeboost in a semi-arid Mediterranean region. Geoderma 286:35–45. http://dx.doi.org/10.1016/j.geoderma.2016.10.019.
Schmolke, A., Thorbek, P., DeAngelis, D.L., Grimm, V., 2010. Ecological models supporting environmental decision making: a strategy for the future. Trends Ecol. Evol. 25: 479–486. http://dx.doi.org/10.1016/j.tree.2010.05.001.
Stockmann, U., Adams, M.A., Crawford, J.W., Field, D.J., Henakaarchchi, N., Jenkins, M., Minasny, B., McBratney, A.B., Courcelles, V. de R., Singh, K., Wheeler, I., Abbott, L., Angers, D.A., Baldock, J., Bird, M., Brookes, P.C., Chenu, C., Jastrow, J.D., Lal, R., Lehmann, J., O'Donnell, A.G., Parton, W.J., Whitehead, D., Zimmermann, M., 2013. The knowns, known unknowns and unknowns of sequestration of soil organic carbon. Agric. Ecosyst. Environ. 164:80–99. http://dx.doi.org/10.1016/j.agee.2012.10.001.
Vaysse, K., Lagacherie, P., 2015. Evaluating Digital Soil Mapping approaches for mapping GlobalSoilMap soil properties from legacy data in Languedoc-Roussillon (France). Geoderma Reg. 4:20–30. http://dx.doi.org/10.1016/j.geodrs.2014.11.003.
Ventrella, D., Fiore, A., Vonella, A.V., Fornaro, F., 2011. Effectiveness of the GAEC cross-compliance standard management of stubble and crop residues in the maintenance of adequate contents of soil organic carbon. Ital. J. Agron. 6:7. http://dx.doi.org/10.4081/ija.2011.6.s1.e7.
Vereecken, H., Schnepf, A., Hopmans, J.W., Javaux, M., Or, D., Roose, T., Vanderborght, J., Young, M.H., Amelung, W., Aitkenhead, M., Allison, S.D., Assouline, S., Baveye, P., Berli, M., Brüggemann, N., Finke, P., Flury, M., Gaiser, T., Govers, G., Ghezzehei, T., Hallett, P., Hendricks Franssen, H.J., Heppell, J., Horn, R., Huisman, J.A., Jacques, D., Jonard, F., Kollet, S., Lafolie, F., Lamorski, K., Leitner, D., McBratney, A., Minasny, B., Montzka, C., Nowak, W., Pachepsky, Y., Padarian, J., Romano, N., Roth, K., Rothfuss, Y., Rowe, E.C., Schwen, A., Šimůnek, J., Tiktak, A., Van Dam, J., van der Zee, S.E.A.T.M., Vogel, H.J., Vrugt, J.A., Wöhling, T., Young, I.M., 2016. Modeling soil processes: review, key challenges, and new perspectives. Vadose Zo. J. 15.
Viola, F., Liuzzo, L., Noto, L.V., Lo Conti, F., La Loggia, G., 2014. Spatial distribution of temperature trends in Sicily. Int. J. Climatol. 34:1–17. http://dx.doi.org/10.1002/joc.3657.
Wang, S., Wang, Q., Adhikari, K., Jia, S., Jin, X., Liu, H., 2016. Spatial-temporal changes of soil organic carbon content in Wafangdian, China. Sustainability 8:1154. http://dx.doi.org/10.3390/su8111154.
Yang, R., Rossiter, D.G., Liu, F., Lu, Y., Yang, F., Yang, F., Zhao, Y., Li, D., Zhang, G., Ryan, M., Law, B., Grimm, R., Behrens, T., Marker, M., Elsenbeer, H., Kheir, R., Greve, M., Bocher, P., Greve, M., Larsen, R., McCloy, K., Martin, M., Wattenbach, M., Smith, P., Meersmans, J., Jolivet, C., Boulonne, L., McBratney, A., Santos, M., Minasny, B., Minasny, B., McBratney, A., Santos, M., Odeh, I., Guyon, B., Malone, B., McBratney, A., Minasny, B., Laslett, G., Vasques, G., Grunwald, S., Comerford, N., Sickman, J., Liu, F., Zhang, G., Sun, Y., Zhao, Y., Li, D., Sullivan, D., Shaw, J., Rickman, D., Vaudour, E., Bel, L., Gilliot, J., Coquet, Y., Hadjar, D., Cambier, P., Coleman, T., Agbu, P., Montgomery, O., Nanni, M., Demattê, J., Demattê, J., Galdos, M., Guimarães, R., Genú, A., Nanni, M., Zullo, J., Huang, X., Senthilkurnar, S., Kravchenko, A., Thelen, K., Qi, J., Jaber, S., Al-Qinna, M., Jobbágy, E., Jackson, R., Shi, Y., Baumann, F., Ma, Y., Song, C., Kühn, P., Scholten, T., Elith, J., Leathwick, J., Hastie, T., Leathwick, J., Elith, J., Francis, M., Hastie, T., Taylor, P., Elith, J., Graham, C., Anderson, R., Dudik, M., Ferrier, S., Guisan, A., Friedman, J., Meulman, J., Carslaw, D., Taylor, P., Froeschke, J., Froeschke, B., Lawrence, R., Bunn, A., Powell, S., Zambon, M., Pouteau, R., Rambal, S., Ratte, J., Gogé, F., Joffre, R., Winkel, T., Krishnan, P., Bourgeon, G., Lo, S.D., Nair, K., Prasanna, R., Srinivas, S., Martin, M., Lo, S.D., Boulonne, L., Jolivet, C., Nair, K., Bourgeon, G., Jalabert, S., Martin, M., Renaud, J., Boulonne, L., Jolivet, C., Montanarella, L., Razakamanarivo, R., Grinand, C., Razafindrakoto, M., Bernoux, M., Albrecht, A., Jafari, A., Khademi, H., Finke, P., Van de Wauw, J., Ayoubi, S., Yang, F., Zhang, G., Yang, J., Li, D., Zhao, Y., Liu, F., Olaya, V., Li, L., Wang, Y., Li, Y., Ye, X., Chu, Y., Wang, X., Wang, Z., Han, X., Chang, S., Wang, B., Yu, Q., Hou, L., Xie, Z., Zhu, J., Liu, G., Cadisch, G., Hasegawa, T., Chen, C., Wang, G., Qian, J., Cheng, G., Lai, Y., Minasny, B., McBratney, A., Malone, B., Wheeler, I., Ma, W., He, J., Yang, Y., Wang, X., Liang, C., Anwar, M., Kirschbaum, M., Bui, E., Henderson, B., Viergever, K., Turner, D., Cohen, W., Kennedy, R., Fassnacht, K., Briggs, J., Riano, D., Chuvieco, E., Salas, J., Aguado, I., Geerken, R., Zaitchik, B., Evans, J., Jin, X., Wan, L., Zhang, Y., Hu, G., Schaepman, M., Clevers, J., Giles, P., Wilson, P., Dare, P., 2015. Predictive mapping of topsoil organic carbon in an alpine environment aided by Landsat TM. PLoS One 10, e0139042. http://dx.doi.org/10.1371/journal.pone.0139042.
Yigini, Y., Panagos, P., 2016. Assessment of soil organic carbon stocks under future climate and land cover changes in Europe. Sci. Total Environ. 557:838–850. http://dx.doi.org/10.1016/j.scitotenv.2016.03.085.
Zinn, Y.L., Lal, R., Resck, D.V.S., 2005a. Changes in soil organic carbon stocks under agriculture in Brazil. Soil Tillage Res. 84:28–40. http://dx.doi.org/10.1016/j.still.2004.08.007.
Zinn, Y.L., Lal, R., Resck, D.V.S., 2005b. Texture and organic carbon relations described by a profile pedotransfer function for Brazilian Cerrado soils. Geoderma 127:168–173. http://dx.doi.org/10.1016/j.geoderma.2005.02.010.